Published in final edited form as:
*Laryngoscope*. 2010 May ; 120(5): 895–901. doi:10.1002/lary.20624.

# Injectable Tissue-Engineered Bone Repair of a Rat Calvarial Defect

**Scott J. Stephan, MD**, **Sunil S. Tholpady, MD, PhD**, **Brian Gross, BS**, **Caren E. Petrie-Aronin, PhD**, **Edward A. Botchway, PhD**, **Lakshmi S. Nair, PhD**, **Roy C. Ogle, PhD**, and **Stephen S. Park, MD**
Department of Otolaryngology–Head & Neck Surgery (S.J.S., B.G., S.S.P.); the Department of Plastic and Reconstructive Surgery (S.S.T., R.C.O.), Department of Biomedical Engineering (C.E.P.-A., E.A.B.), and the Department of Orthopaedic Surgery (L.S.N.), University of Virginia, Charlottesville, Virginia, U.S.A.

## Abstract

**Objectives/Hypothesis—**Advances in bone repair have focused on the minimally-invasive delivery of tissue-engineered bone (TEB). A promising injectable biopolymer of chitosan and inorganic phosphates was seeded with mesenchymal stem cells (MSCs) and a bone growth factor (BMP-2), and evaluated in a rat calvarial critical size defect (CSD). Green fluorescent protein (GFP)-labeled MSCs are used to evaluate patterns of cell viability and proliferation.

**Study Design—**Prospective, controlled trial in an animal model.

**Methods—**In 30 male rats, 8-mm calvarial CSDs were created, and divided into five groups of six animals each. In the experimental groups, the defects were injected with either chitosan gel, gel loaded with MSCs ($0.3 \times 10^6$ cells/defect), gel loaded with BMP-2 (2 μg/defect), or gel loaded with both MSC and BMP-2. In the control group, the defect was left untreated. At 4 weeks, in vivo microcomputed tomography (micro-CT) analysis was performed. At 8 weeks, calvarial specimens were examined by micro-CT, histology, and immunohistochemistry.

**Results—**New areas of bone growth were seen in the defects of all treated animals. Micro-CT analysis revealed a significant ($P < .001$) time-dependent increase in the regeneration of bone volume and bone area in defects treated with gel/MSC/BMP-2 as compared to all other groups. Histological analysis confirmed this difference. GFP–labeled TEB was detected within the areas of new bone, indicating cell viability and contribution to new bone growth by the injected MSC.

**Conclusions—**This study demonstrates that an injectable form of TEB using a chitosan gel, MSC, and BMP-2 can enhance bone formation in a rat calvarial CSD.

### Keywords

Bone regeneration; chitosan; bone morphogenetic protein; cranial defect; mesenchymal stem cell

## INTRODUCTION

The repair of craniofacial bony defects is surgically challenging due to the delicate and complex anatomy of the craniofacial skeleton. Autografts, allografts, and synthetic bone



Send correspondence to Scott J. Stephan, MD, Department of Otolaryngology–Head and Neck Surgery, University of Virginia, PO Box 800713, Charlottesville, VA 22908. scott.stephan@virginia.edu.

Presented at the Triological Society Combined Otolaryngology Spring Meeting, Phoenix, Arizona, U.S.A., May 28–31, 2009.

substitutes have been used with variable success, each having distinct disadvantages that limit their clinical application. One focus of craniofacial reconstructive research has been the use of tissue-engineered bone (TEB) as a promising alternative to implantable materials. The ideal TEB would allow regeneration and integration of bone in a minimal span of time. It would be nonreactive, nonimmunogenic, easily delivered, and produce long-lasting structural bone. One strategy in the development of TEB is the use of a biodegradable polymer as a temporary three-dimensional scaffold to allow for the delivery of bioactive materials and progenitor cells to participate in organized bone regeneration.[1–3]

A variety of natural and synthetic biomaterials have been used to mimic extracellular matrix and serve as scaffolds for new tissue formation. The majority of cell-based therapies have employed solid, implantable constructs that are preformed and require an open procedure for delivery of TEB.[4–6] The ability to produce TEB with an injectable polymer would provide tremendous potential as a minimally invasive way to repair or recontour craniofacial defects that offers several key advantages over implanted polymer scaffolds. A fluid material can fill any shaped defect, may incorporate various growth factors, need not contain residual solvents, such as those in preformed scaffolds, and does not require an open surgical procedure for placement.

Bone morphogenetic proteins (BMP) are known to have the ability to stimulate differentiation of uncommitted mesenchymal stem cells (MSCs) along the osteogenic lineage and enhance the function of differentiated osteoblasts.[7] The first indication of their existence was the ability of demineralized bone matrix to produce ectopic bone when implanted in vivo.[8] Since that time, over 20 BMPs have been discovered. They are multifactorial and belong to the transforming growth factor superfamily of growth factors. As such, they are implicated in multiple developmental processes and are critical for bone regeneration.

One member of this growth factor family, BMP-2, has been shown to accelerate bone healing in a number of animal models.[7] BMP-2 has a short half-life in vivo and requires a suitable carrier matrix, such as a biopolymer gel, to maintain significant activity in vivo.[9]

A promising biopolymer made of chitosan, a natural biopolymer derived from crustacean exoskeleton, has been the focus of current biomedical research for its many interesting clinical applications. An injectable thermogelling solution made of chitosan and inorganic phosphates that is cytocompatible with osteoprogenitor cells was recently developed at our institution. It can deliver bioactive materials effectively and forms a gel at physiologic temperatures.[10] The unique properties of this chitosan biopolymer hold potential as a practical and effective carrier matrix for the delivery of TEB.

In this study, TEB was generated by a thermogelling chitosan solution seeded with MSC and BMP-2 delivered by in vivo injection to critical size rat calvarial defects. Radiographic, histologic, and immunohistochemical analysis were used to evaluate bone regeneration.

## MATERIALS AND METHODS

### Overview

MSC from the bone marrow of adult green fluorescent protein (GFP)-labeled rats were harvested and cultured in osteogenic medium. A mixture of MSC, BMP-2, and chitosan gel was injected into critical size defects (CSDs) created in the calvaria of adult rats. The animal protocol was reviewed and approved by the University of Virginia Animal Care and Use Committee. All animals were housed and received veterinary care in the vivarium at the University of Virginia. At 4 weeks, in vivo microcomputed tomography (micro-CT) scans

were obtained of the calvarial defects. At 8 weeks, the calvaria were harvested and ex vivo high-resolution micro-CT scans were obtained of the defects. The defects were analyzed for histological and immunohistochemical properties.

### Harvest of Mesenchymal Stem Cells

Sprague-Dawley rats, 6–8 months old, previously engineered to express a single copy of enhanced green fluorescent protein (GFP), were sacrificed by intracardiac lidocaine injection. The purpose of harvesting labeled cells from this animal line was to then implant them into wild type Sprague-Dawley rats not expressing GFP to follow the fate of the implanted cells. In a sterile fashion, the femurs were dissected free from the surrounding soft tissue, severed at midshaft, and centrifuged (10,000 rpm) to extract the bone marrow containing MSCs. The cells were maintained in culture as previously described.[11] Briefly, MSCs were maintained in a medium of Dulbecco's Modified Eagle's Medium (DMEM) with high glucose and containing 10% fetal bovine serum, 1 μg/mL gentamicin, 2 mmol/L glutamine, 1 mmol/L nonessential amino acid (Life Technologies, Gaithersburg, MD), insulin, transferrin, and selenium (Collaborative Biomedical Products, Bedford, MA). Cells were cultured in 100-mm culture dishes in a humidified, mixed environment of 5% $CO_2$/95% air at 37°C. Second-passage cells were displaced off the cell culture plates via trypsin digestion and placed in DMEM at a concentration of $12.5 \times 10^5$ cells/30 μL DMEM.

### Synthesis of Chitosan Construct

Chitosan from crab shells (minimum 85% deacetylation) and ammonium hydrogen phosphate (AHP) were procured from Sigma (St. Louis, MO). As previously described,[10] chitosan was dissolved in 0.5% acetic acid solution (~2.8%) under magnetic stirring for 48 hours at room temperature. The resulting solution (pH ~5.6) was filtered and stored at 4°C. The viscosity of the solution was found to be 5,300 cps when measured at a shear rate of 4 $s^{-1}$ (Brookfield DV-IIþ Pro Viscometer; Brookfield Engineering Laboratories, Inc., Middleboro, MA). Chitosan (5 mL) was aliquoted into a glass vial and magnetically stirred in an ice bath. AHP solution (60% in water, pH ~8.6) was slowly added to the chilled chitosan solution. The pH of the resulting mixture was found to be in the range of 7 to 7.2.

### Delivery of Chitosan/BMP/MSC Construct

Thirty adult male Sprague-Dawley rat retired breeders (400–550 g) were randomly assigned to five different experimental groups: control, gel only, BMP/gel, MSC/gel, and BMP/MSC/gel. Animals were intraperitoneally anesthetized using 4.5 mg/100 g Nembutal. The head was shaved, sterilized with Betadine and 70% ethanol, and mounted onto a stereotactic restraint. An incision was made midline from the supraorbital glabella to the occiput. This incision was taken through the periosteum, which was elevated from the underlying bone and retracted laterally. A bone-cutting burr was used to create 8-mm calvarial defects to the level of the dura and sigmoid sinus. Sterile saline solution was used to keep membranes moist and to thoroughly remove bone debris. After the osseous defect was created, a 1-mL syringe with a 19-gauge needle loaded with 300 μL of biopolymer construct (chitosan-AHP solution with or without MSC or BMP) was delivered into the center of the defect. In cell-treated groups, $0.3 \times 10^6$ MSC pellet was resuspended in chitosan solution to a total volume of 300 μL loaded in a syringe and injected into the defect. For those groups treated with BMP, 4 μg of growth factor (500 μg/mL) was added to chitosan solution to a total of 300 μL and injected into the defect. The periosteum was then closed with 6-0 nylon around the needle exiting from the distal portion of the incision. Then entire volume of construct was then injected into the defect. The skin was closed with 4-0 absorbable suture. Both antibiotics and analgesics were administered for 1 week following surgery.

### Microcomputed Tomography Analysis

Bone formation in animals was followed over an 8-week time course. A quantitative microcomputed tomography specimen imaging scanner (Scanco, Bassersdorf, Switzerland) was used to assess new bone formation in the defect at 4 weeks in vivo and 8 weeks ex vivo. At 4 weeks, all animals were anesthetized by intraperitoneal injection of 4.5 mg/100 g Nembutal and imaged utilizing a low-resolution 45 kVp scan. All animals were sacrificed at 8 weeks and ex vivo scans of each specimen were obtained utilizing a high-resolution 45 kVp scan. Following reconstruction of the 2-dimensional (2D) slices, an appropriate threshold matching the original grayscale images was chosen. Contour lines were drawn around the defect area to appropriately select a circular defect void volume of 8 mm × 1 mm, taking care to exclude neighboring native bone. Three-dimensional (3D) images were created from 2D slices, and the bone volume within the selected circular defect was calculated using the 3D evaluation program. Bone void volume, threshold (160), and scan parameters (support = 4; width = 1.2) were kept constant throughout the entire study. In addition, micro-CT–based morphometric analyses of defects were used to determine the area within the defect covered by new bone formation, using Image-Pro Plus version 5.0 (Media Cybernetics, Carlsbad, CA).

### Histological Analysis

Following micro-CT scanning, each sample was decalcified in 10% ethylenediaminetetraacetic acid (EDTA) (Richard Scientific, Kalamazoo, MI) for 2 weeks at room temperature on a rotating rocker. Following decalcification, samples were dehydrated overnight. Samples were then cut along the coronal plane at the midline of the defect and embedded in paraffin. Sections at 7 μm each were mounted onto individual slides, and stained with hematoxylin and eosin. Representative samples were evaluated for new bone formation, bone architecture, and inflammatory markers.

### Immunohistochemical Analysis

Paraffin-embedded decalcified bone sections were processed for immunohistochemistry using a primary rabbit anti-GFP antibody (Santa Cruz Biotechnology, Santa Cruz, CA) and a goat anti-rabbit antibody conjugated to avidin-biotin and developed with peroxidase using the manufacturer's protocols (Vector Laboratories, Burlingame, CA). Primary antibody was diluted 1:100 and secondary 1:500 in 5% goat serum. Peroxidase activity was visualized with diaminobenzidine (Sigma, St. Louis, MO). Images were acquired using an inverted microscope (model BX51; Olympus, Tokyo, Japan) equipped with a digital camera (model DP70; Olympus) using Adobe Photoshop software (Adobe, San Jose, CA).

### Statistical Analysis

GraphPad Prism (GraphPad Software, La Jolla, CA) was used to perform a 1-way analysis of variance test to measure statistical significance when comparing experimental groups. Significance was asserted at $P < .05$.

## RESULTS

### Bone Healing in a Rat Cranial CSD

Evaluation of the osteogenic potential of the TEB construct was performed at distinct time points over an 8-week period. The TEB, composed of chitosan and a combination of either BMP and/or MSC, was placed into critical size defects and subjected to micro-CT analysis. This analysis was performed in vivo at 4 weeks and ex vivo at the end of the experiment (8 weeks). Micro-CT–guided morphometric analyses quantified the area within the defect

covered by new bone formation. This quantification accompanied the qualitative data regarding the location of new regenerating bone.

Figure 1 demonstrates representative samples of each of the five groups as assessed by micro-CT at 4 and 8 weeks. Aside from the control (untreated) group, each group consistently demonstrates greater density of bone regeneration at 8 weeks when compared to 4 weeks. Additionally, this volume appears to increase linearly, with the amount of bone present at the first time point virtually doubling at the second time point.

Qualitative analysis also shows an increase in bone with the addition of BMP and/or MSC when compared to the control or gel-only groups. The combination of BMP and MSC appears to act synergistically to produce continual healing over the study period. Although the MSC/gel group appears to regenerate bone better than the BMP/gel group, the addition of both produces a construct that regenerates more bone at 4 weeks than all other groups at 8 weeks.

Another salient visual result is the location of bone formation. Although minimal bone regeneration occurs in the control and gel groups, this sparse bone was localized to the periphery of the defect. This pattern of bone formation was also observed in the BMP/gel group. The remaining two groups containing MSC displayed central and peripheral healing. This pattern was more pronounced in the BMP/MSC/gel group, but also was true of the MSC/gel group.

Quantification of bone regeneration via morphometric analysis confirms qualitative conclusions. As can be seen in Figure 2, a significant difference exists in each group between the quantity of bone regenerated at 4 and 8 weeks (except for the defect-only control group). No statistically significant difference was found between the gel alone, BMP/gel, and MSC/gel groups, either at the 4 week or 8 week time points. This is in stark contrast to the BMP/MSC/gel group, which had significant bony healing at 4 and 8 weeks. The amount of bone healing seen at 4 weeks for this group exceeded the regeneration present at 8 weeks for any other group. The analysis also revealed quantitatively that the amount of bone created at the end of 8 weeks was approximately three times more in the group that received both BMP and MSC as compared to all other groups (Fig. 3). This again confirms the synergistic effect seen qualitatively.

### Histologic and Immunohistochemical Analysis

Histologic assessment of the osteogenic potential of TEB was performed at the experimental end. Hematoxylin and eosin-stained sections were analyzed with light microscopy at various levels of magnification yielding information on the quality and histologic characteristics of bone regeneration, implanted chitosan gel, and surrounding cell infiltrate.

At the end of the experimental period, residual gel was seen within all defects after 8 weeks. The gel alone group had a minimal amount of bone formation, but did contain large amounts of unresorbed gel. In the other groups, the majority of gel was resorbed and the remainder was seen in many areas to be mixed with blood and fibrin. A greater degree of gel resorption was observed in the BMP/gel group, as compared with gel-alone or either cell-treated group (MSC/gel, BMP/MSC/gel). In the two cell-treated groups, chitosan gel is found at the interphase of newly formed immature bone (Fig. 4). Although large areas of the gel in the cell-treated groups were devoid of cells, areas of new bone formation where characterized by incorporation of osteoprogenitor cells within the gel (Fig. 4).

Islands of bone formation histologically correspond well to micro-CT data obtained. Bone was seen in all groups of treated animals, with a thin layer of bone almost completely

covering the defect of the BMP/MSC/gel group. This bone appeared to be present both in the periphery and the center, as opposed to other groups. The BMP/gel group additionally had a much more vigorous cellular response at the bone-defect interface, as evidenced by the multiple spindle shaped cells with a high nucleus:cytoplasmic ratio (Fig. 4).

Utilization of specifically labeled MSC allowed for the unique opportunity to determine the presence or absence of surviving progeny within the defects. Immunohistochemical staining for GFP-localized viable MSC was shown using a brown colorimetric reaction (Fig. 5). Defects containing BMP/MSC/gel constructs were seen histologically to contain the largest number of GFP-positive cells. These cells were present within the osteoid and along newly forming bone, indicating the MSCs had converted to osteoblasts and were secreting bone. The specificity of the stain can also be appreciated as defects containing BMP/gel did not contain any background staining (Fig. 5).

## DISCUSSION

The clinical challenge encountered in the reconstruction of craniofacial bony defects has prompted multiple modalities to repair these defects. These include autografts, allografts, and tissue-engineered constructs. All modalities have inherent disadvantages; clinical knowledge and experience dictate their use. Autografts use tissue from the patient to reconstruct defects at a distant location, but this can be complicated by donor-site morbidity, infection, and an extra incision with concomitant pain. Allografts overcome some of these problems, but can also be a source of infectious vector transmission, poor incorporation, and extrusion. [12,13] Tissue-engineered constructs are becoming more common, but do not contain purified cells and usually consist of growth factor(s) contained within a carrier.

In this study, elements known to be relevant for inducing and accelerating bony growth were placed into a gel with unique properties. The goal is to use a gel with osteoconductive and osteoinductive properties that would have clinical advantages over current treatment modalities. The base carrier, chitosan gel, is a well-characterized biomaterial derived from the exoskeleton of crustaceans. Its most common use in humans involves hemostasis in battlefield injuries.[14] Although not clinically osteoconductive, it can serve as an adequate carrier for cells and growth factors.[15,16] Here we confirm previous results and demonstrate that chitosan gel alone does not promote significantly greater healing than the control group (Fig. 2).

The base chitosan gel was augmented with BMP-2 and/or MSC to evaluate bony healing. These both have been individually shown to augment bone formation. As stated before, BMP-2 is a member of the multifunctional transforming growth factor superfamily, most commonly associated with bone formation and regeneration.[9]

The MSC utilized in this study are among the best characterized adult stem cells present within the mammalian organism.[17] These cells are relatively uncommitted cells derived from a fibroblastic, tissue culture plastic adherent, nonhematopoietic cell population residing in bone marrow. They have the capacity to express markers of other tissue types, including muscle, [17] nerve,[18] fat,[19] and cartilage.[20] Implantation of the cells has the potential to enhance healing of bone,[21,22] cartilage,[23] and tendon,[24,25] as seen in other studies.

These cells are not located solely in the hematopoietic niche. Adult stem cells have been identified in fat,[26] muscle,[27] dura,[28] and other locations. All appear to be fibroblastic cells capable of displaying gene products of tissues derived from mesoderm, ectoderm, and interestingly, endoderm. Future studies will likely incorporate the other adult stem cells for contrast and comparison with marrow mesenchymal cells.

The model used for this study was the critical size rat calvarial defect.[29] The critical size defect is a model independently validated for each and every defect and animal. It represents the smallest size defect that will heal less than 10% over the lifetime of the animal. Using this model, the difference, however small, is directly related to the implant material and not to the innate regenerative capacity of the study animal.

The coverage of the defect with bone was not an unexpected event, especially with the addition of cells and a growth factor accelerant. The result that was unexpected, however, was the near equivalency of bone healing between the BMP/gel and MSC/gel groups. A priori conjecture as to the relative levels of bone healing between the two groups could lead to conclusions that are logically sound, but ultimately wrong. The BMP group increased the amount of bone formation at the periphery of the defect, whereas the MSCs provided a supply of cells and elaborated factors that created bone closer to the center. At the end of 8 weeks, both of these groups provided a nonsignificant increase in bone healing above gel alone.

Addition of both BMP and MSC to the defect site acted in a greater than additive fashion to enhance bone healing. Many explanations can be formulated for this result. BMP likely enhanced peripheral bone formation, but also provided a factor known to convert MSC to osteoblasts. The MSCs also generate growth factors responsible for angiogenesis. Thus, before the MSC conversion to osteoblasts, it is likely that the signals required for angiogenesis were present and ready to revascularize the nascent island of bone.

A major limitation to regeneration of bone is the relative lack of a vascular supply. A diffusion barrier exists beyond which cells are unable to obtain nutrients via plasmatic imbibition. This problem is exacerbated in bone, where formation of osteoid can lead to death of the cells producing and encasing themselves in osteoid. Thus, much of the bone that is produced has a limited diameter directly related to the size at which the cells cannot support themselves through diffusion.

Histologic analysis complemented the micro-CT findings of bone formation within defects. Cross-sectional analysis of the defects demonstrated a greater amount of bone growth centrally in those defects containing MSC than those without MSC. The addition of BMP increased the cellularity at the bone defect junction, likely due to its proliferative effect on osteoblasts.

In addition to bone formation, the model used allowed identification of implanted cells or their progeny. The MSC were derived from a rat line constitutively expressing GFP. The detection of GFP via fluorescent microscopy was not viable in this system secondary to the background fluorescence of bone and the diminishment of signal due to fixation and decalcification. Immunohistochemistry directed at GFP clearly demonstrated cytoplasmic staining present within cells encased in osteoid, presumably osteoblasts. This finding further supports the inference that MSCs convert to osteoblasts due to the action of BMP-2.

## CONCLUSION

This set of studies demonstrates the viability of a cell/growth factor/carrier construct in the minimally invasive delivery of a bone forming construct. Delivery of this construct was simple and produced bone detectable histologically and by computed tomography. Clinically this combination could be easily produced and delivered operatively or in a minimally invasive clinical setting for the treatment of bony deficits. Future experiments will utilize other adult stem cells and growth factor combinations that will enhance angiogenesis and osteogenesis.

## Acknowledgments

We would like to thank Rebecca Ogle for assistance with cell isolation and propagation, and maintenance of the GFP rat colony. We are grateful to the American Society of Pediatric Otolaryngology for the funding and support provided in the C.O.R.E. Grant Program, 2008.

This work was supported by the Centralized Otolaryngology Research Efforts (CORE) Grant Program, American Society of Pediatric Otolaryngology, 2008.

## BIBLIOGRAPHY

1. Persidis A. Tissue engineering. Nat Biotechnol. 1999; 17:508–510. [PubMed: 10331816]
2. Service RF. Tissue engineers build new bone. Science. 2000; 289:1498–1500. [PubMed: 10991738]
3. Petite H, Viateau V, Bensaid W, et al. Tissue-engineered bone regeneration. Nat Biotechnol. 2000; 18:959–963. [PubMed: 10973216]
4. Li ZS, Ramay HR, Hauch KD, Xiao DM, Zhang MQ. Chitosan-alginate hybrid scaffolds for bone tissue engineering. Biomaterials. 2005; 26:3919–3928. [PubMed: 15626439]
5. Mukherjee DP, Tunkle AS, Roberts RA, Clavenna A, Rogers S, Smith D. An animal evaluation of a paste of chitosan glutamate and hydroxyapatite as a synthetic bone graft material. J Biomed Mater Res B Appl Biomater. 2003; 67B:603–609. [PubMed: 14528457]
6. Yoon E, Dhar S, Chun DE, Gharibjanian NA, Evans GRD. In vivo osteogenic potential of human adipose-derived stem cells/polylactide-co-glycolic acid constructs for bone regeneration in a rat critical-sized calvarial defect model. Tissue Eng. 2007; 13:619–627. [PubMed: 17518608]
7. Sawyer AA, Song SJ, Susanto E, et al. The stimulation of healing within a rat calvarial defect by mPCL-TCP/collagen scaffolds loaded with rhBMP-2. Biomaterials. 2009; 30:2479–2488. [PubMed: 19162318]
8. Huggins C, Wiseman S, Reddi AH. Transformation of fibroblasts by allogeneic and xenogeneic transplants of demineralized tooth and bone. J Exp Med. 1970; 132:1250–1258. [PubMed: 4929179]
9. Toriumi DM, Robertson K. Bone inductive biomaterials in facial plastic and reconstructive surgery. Facial Plast Surg. 1993; 9:29–36. [PubMed: 8472967]
10. Nair LS, Starnes T, Ko JW, Laurencin CT. Development of injectable thermogelling chitosan-inorganic phosphate solutions for biomedical applications. Biomacromolecules. 2007; 8:3779–3785. [PubMed: 17994699]
11. Wong GL, Cohn DV. Target cells in bone for parathormone and calcitonin are different: enrichment for each cell type by sequential digestion of mouse calvaria and selective adhesion to polymeric surfaces. Proc Natl Acad Sci USA. 1975; 72:3167–3171. [PubMed: 171656]
12. Suchanek W, Yoshimura M. Processing and properties of hydroxyapatite-based biomaterials for use as hard tissue replacement implants. J Mater Res. 1998; 13:94–117.
13. Burg KJL, Porter S, Kellam JF. Biomaterial developments for bone tissue engineering. Biomaterials. 2000; 21:2347–2359. [PubMed: 11055282]
14. Ishihara M, Ono K, Sato M, et al. Acceleration of wound contraction and healing with a photocrosslinkable chitosan hydrogel. Wound Repair Regen. 2001; 9:513–521. [PubMed: 11896994]
15. Park DJ, Choi BH, Zhu SJ, Huh JY, Kim BY, Lee SH. Injectable bone using chitosan-alginate gel/mesenchymal stem cells/BMP-2 composites. J Craniomaxillofac Surg. 2005; 33:50–54. [PubMed: 15694150]
16. Park DJ, Choi JH, Leong KW, Kwon JW, Eun HS. Tissue-engineered bone formation with gene transfer and mesenchymal stem cells in a minimally invasive technique. Laryngoscope. 2007; 117:1267–1271. [PubMed: 17507830]
17. Pittenger MF, Mackay AM, Beck SC, et al. Multilineage potential of adult human mesenchymal stem cells. Science. 1999; 284:143–147. [PubMed: 10102814]
18. Woodbury D, Schwarz EJ, Prockop DJ, Black IB. Adult rat and human bone marrow stromal cells differentiate into neurons. J Neurosci Res. 2000; 61:364–370. [PubMed: 10931522]

19. Sekiya I, Larson BL, Vuoristo JT, Cui JG, Prockop DJ. Adipogenic differentiation of human adult stem cells from bone marrow stroma (MSCs). J Bone Miner Res. 2004; 19:256–264. [PubMed: 14969395]

20. Sekiya I, Vuoristo JT, Larson BL, Prockop DJ. In vitro cartilage formation by human adult stem cells from bone marrow stroma defines the sequence of cellular and molecular events during chondrogenesis. Proc Natl Acad Sci USA. 2002; 99:4397–4402. [PubMed: 11917104]

21. Bruder SP, Kurth AA, Shea M, Hayes WC, Jaiswal N, Kadiyala S. Bone regeneration by implantation of purified, culture-expanded human mesenchymal stem cells. J Orthop Res. 1998; 16:155–162. [PubMed: 9621889]

22. Bruder SP, Jaiswal N, Ricalton NS, Mosca JD, Kraus KH, Kadiyala S. Mesenchymal stem cells in osteobiology and applied bone regeneration. Clin Orthop Relat Res. 1998; 355 suppl:S247–S256. [PubMed: 9917644]

23. Wakitani S, Goto T, Pineda SJ, et al. Mesenchymal cell-based repair of large, full-thickness defects of articular cartilage. J Bone Joint Surg Am. 1994; 76:579–592. [PubMed: 8150826]

24. Young RG, Butler DL, Weber W, Caplan AI, Gordon SL, Fink DJ. Use of mesenchymal stem cells in a collagen matrix for Achilles tendon repair. J Orthop Res. 1998; 16:406–413. [PubMed: 9747780]

25. Awad HA, Butler DL, Boivin GP, et al. Autologous mesenchymal stem cell-mediated repair of tendon. Tissue Eng. 1999; 5:267–277. [PubMed: 10434073]

26. Zuk PA, Zhu M, Mizuno H, et al. Multilineage cells from human adipose tissue: implications for cell-based therapies. Tissue Eng. 2001; 7:211–228. [PubMed: 11304456]

27. Peault B, Rudnicki M, Torrente Y, et al. Stem and progenitor cells in skeletal muscle development, maintenance, and therapy. Mol Ther. 2007; 15:867–877. [PubMed: 17387336]

28. Gagan JR, Tholpady SS, Ogle RC. Cellular dynamics and tissue interactions of the dura mater during head development. Birth Defects Res C Embryo Today. 2007; 81:297–304. [PubMed: 18228258]

29. Sweeney TM, Opperman LA, Persing JA, Ogle RC. Repair of critical size rat calvarial defects using extracellular matrix protein gels. J Neurosurg. 1995; 83:710–715. [PubMed: 7545744]

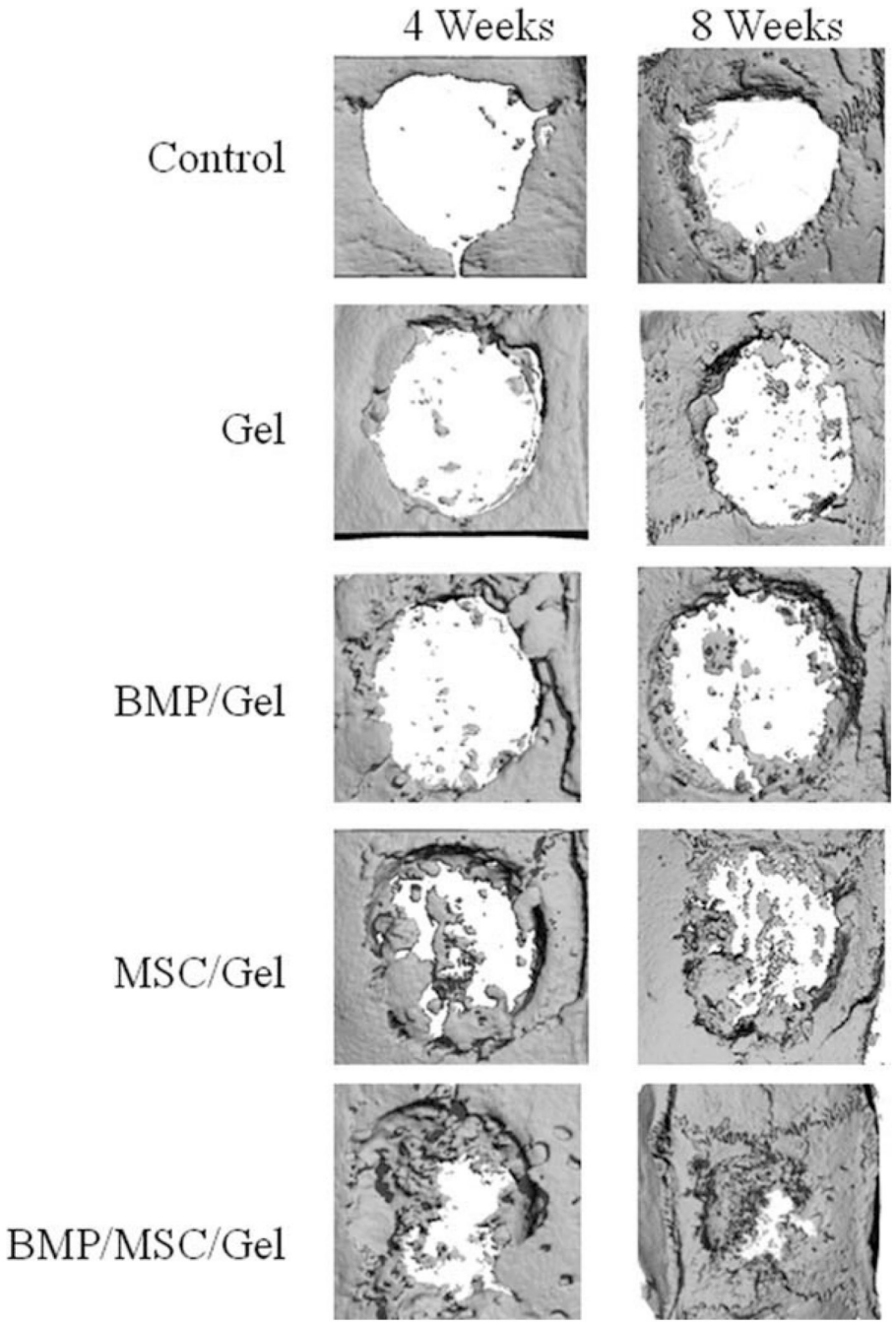


**Fig. 1.**
Micro-CT analysis of cranial defects stratified by groups over the study period. MBP = bone morphogenetic proteins; MSC = mesenchymal stem cells.

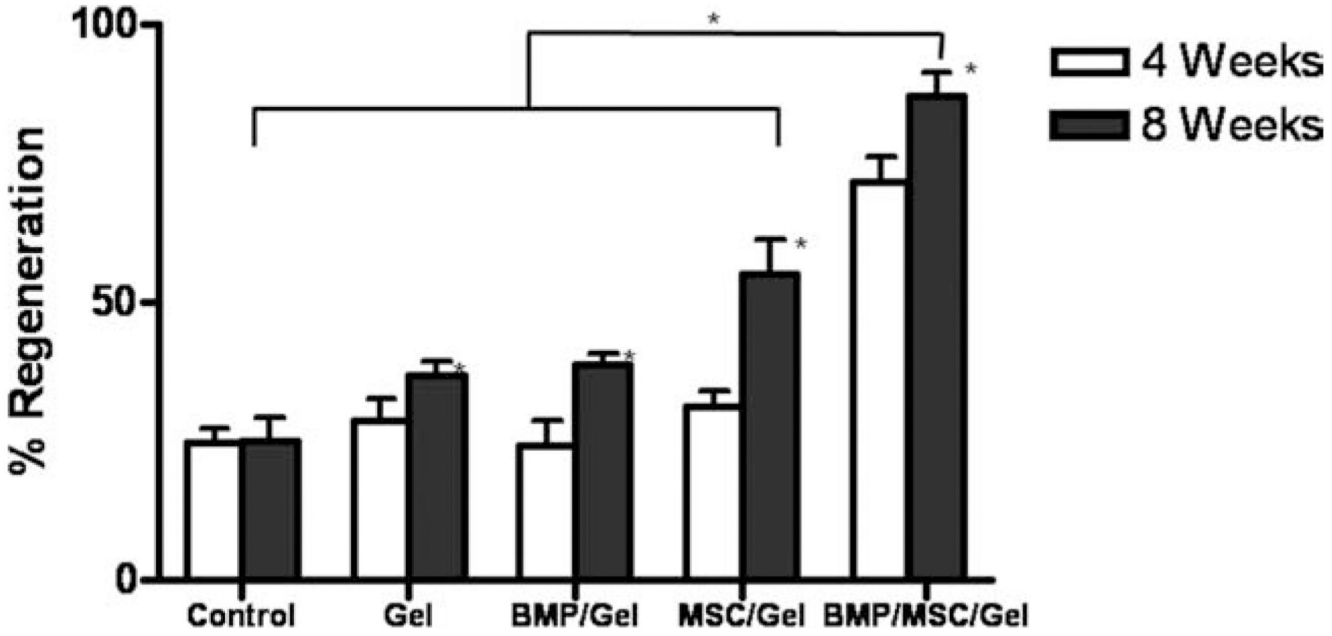


**Fig. 2.**

Percent bone regeneration by area within defects as measured by micro-CT at 4 and 8 weeks. Note the increase in bone regenerated over the study time period. **P* < .05. MBP = bone morphogenetic proteins; MSC = mesenchymal stem cells.

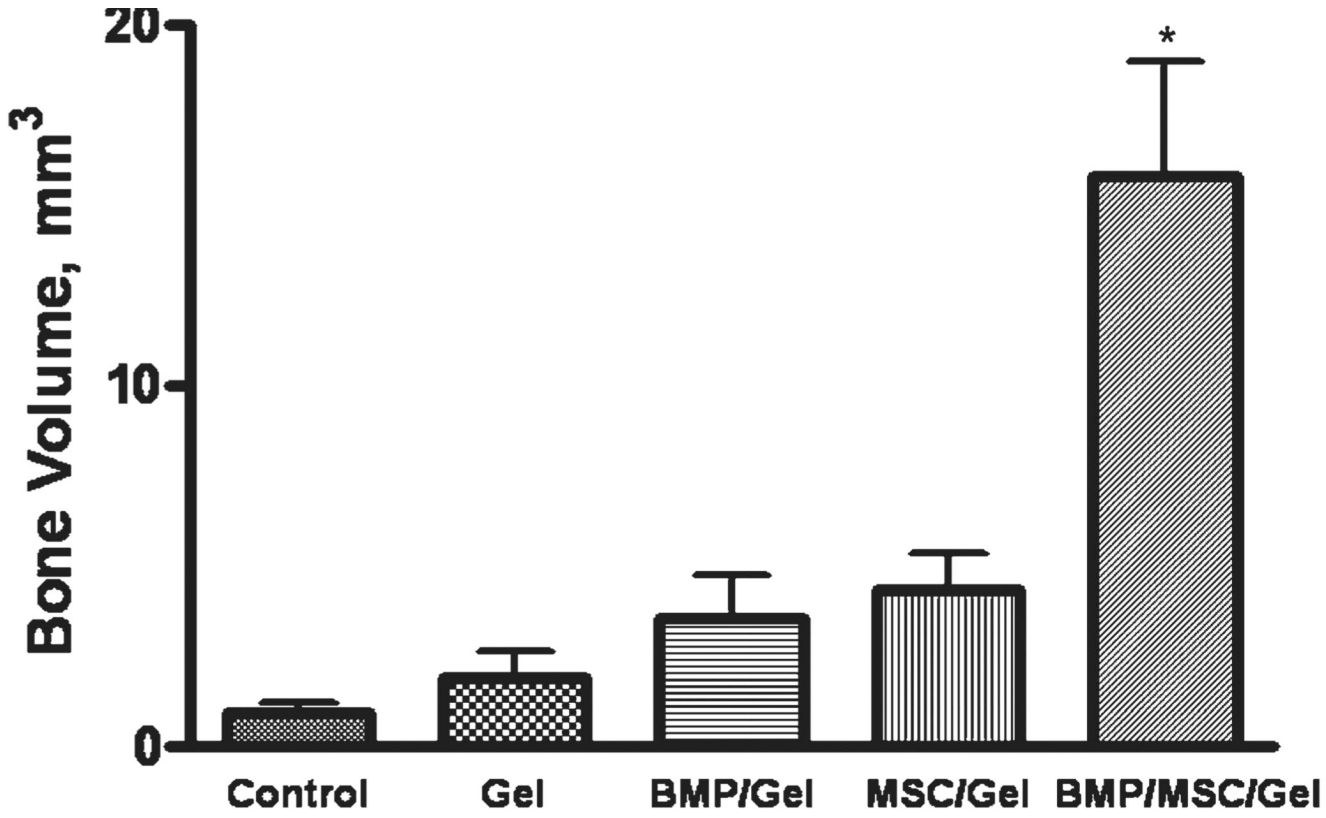


**Fig. 3.**
Calculations of bone volume at 8 weeks within each study group. *$P < .05$. MBP = bone morphogenetic proteins; MSC = mesenchymal stem cells.

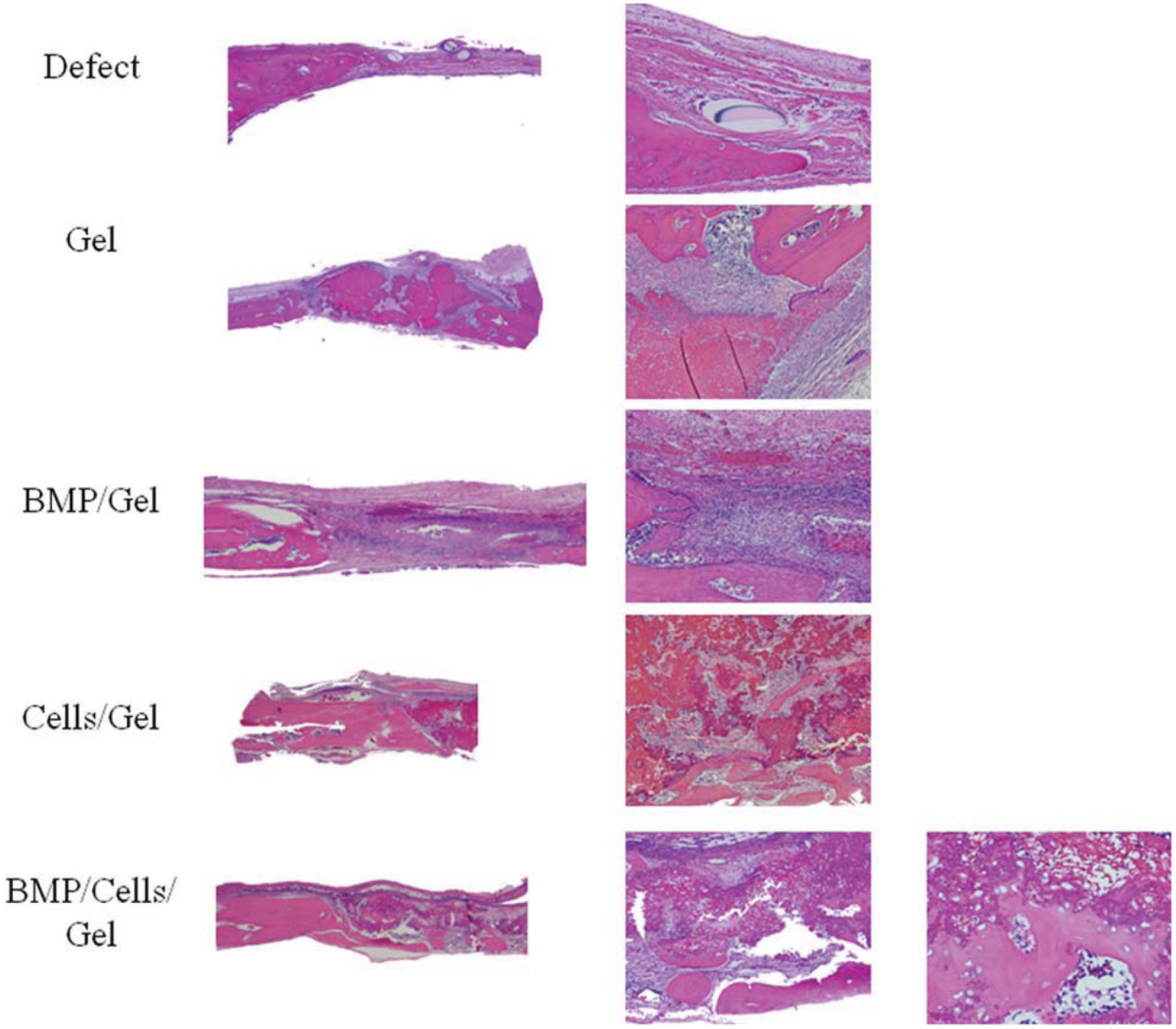


**Fig. 4.**

Hematoxylin and eosin staining of calvarial histologic sections after 8 weeks. Representative sections from each study group shown. MBP = bone morphogenetic proteins. [Color figure can be viewed in the online issue, which is available at www.interscience.wiley.com.]

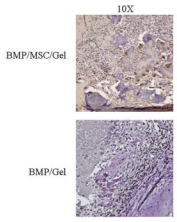


**Fig. 5.**
Immunohistochemistry for green fluorescent protein within mesenchymal stem cells (MSC) implanted into defects. Note lack of staining in defects containing no cells. [Color figure can be viewed in the online issue, which is available at www.interscience.wiley.com.]